SOILS2SEA DELIVERABLE NO. 2.4

BONUS
SCIENCE FOR A BETTER FUTURE OF THE BALTIC SEA REGION

# Scenario analyses for spatially differentiated P measures in catchments

SOILS2SEA

Reducing nutrient loadings from agricultural soils to the Baltic Sea via groundwater and streams

This page has intentionally been left blank

**SOILS2SEA DELIVERABLE NO. 2.4**

# Scenario analyses for spatially differentiated P measures in catchments

**March 2018**

Author: Goswin Heckrath, Nils Onnen, Lorenzo Pugliese, Adrian Pop, Bo V. Iversen, Department of Agroecology, Aarhus University

SOILS2SEA

Reducing nutrient loadings from agricultural soils to the Baltic Sea via groundwater and streams

This report is a publicly accessible deliverable of the Soils2Sea project. The present work has been carried out within the project 'Reducing nutrient loadings from agricultural soils to the Baltic Sea via groundwater and streams (BONUS Soils2Sea)', which has received funding from BONUS, the joint Baltic Sea research and development programme (Art 185), funded jointly from the European Union's Seventh Framework Programme for research, technological development and demonstration and from Innovation Fund Denmark, The Swedish Environmental Protection Agency (Naturvådsverket), The Polish National Centre for Research and Development, The German Ministry for Education and Research (Bundesministerium für Bildung und Forschung), and The Russian Foundation for Basic Research (RFBR).



Heckrath G, Onnen N, Pugliese L, Pop A, Iversen, BV, Scenario analyses for spatially differentiated P measures in catchments. BONUS SOILS2SEA Deliverable 2.4. Department of Agroecology, Aarhus University, Denmark, March 2018, www.Soils2Sea.eu

# Table of Contents

# 1 Background and objectives

Phosphorus (P) losses from agricultural land to surface waters may contribute to eutrophication and hence pose a threat to the aquatic environment. If Denmark is to achieve the EU Water Framework Directive goals of good ecological status in surfaces waters, agricultural P losses have to be reduced markedly (Andersen et al., 2016). This calls for targeted mitigation efforts that address both the source, i.e. P applications to farmland and the soil P pool, and the transport processes of P to water (Kronvang et al., 2009; Schoumans et al., 2014). One prerequisite for effective mitigation is a robust, spatially differentiated assessment of the risk of P losses.

For the example of the Fensholt catchment, this report explores which information with practical relevance for risk assessment is generally available in Denmark and how it relates to measured P losses. Additionally, we analyzed scenarios of land use and climate change for the risk of soil erosion as well as sediment and P delivery to streams. Specifically the objectives are i) to briefly describe spatial data that are typically used for assessing the risk of P loss at the field scale; ii) to model the effect of changed land use, cropping and rainfall on soil redistribution; and iii) to summarize P losses from the Fensholt catchment during the monitoring period May 2015 to April 2017. We consider two main pathways of P transfer from soil to water, namely water erosion (Heathwaite and Dils, 2000) and subsurface runoff in the form of artificial land drainage (King et al., 2015). The data presented were acquired by different research projects (e.g. BONUS SOILS2SEA; iDRÆN www.idraen.dk) and have been compiled as an activity under the BONUS SOILS2SEA project.

# 2 Site description and P source

The Fensholt catchment is located in the moraine landscape of eastern Jutland, Denmark, and some of its characteristics have been described previously (e.g. De Schepper et al. 2017). The Fensholt catchment is a headwater catchment in the western part of the Norsminde catchment (Olesen et al. 2017) for which land use and climate change scenarios have been analyzed. In summary, the hydrological catchment at Fensholt extends over 606 ha. In 2016, agricultural land covered about 80% of the catchment and comprised 122 fields that were at least partly within the catchment. The total area of those fields was 607 ha, of which 42 ha were grassland. Hence, arable agriculture is predominant with a large proportion of winter cereals and spring barley. Additionally, there were 5 ha herbaceous riparian buffer zones and 56 ha forest (Fig. 1). While crop rotations are very similar to the rest of the Norsminde catchment, the proportion of agricultural was notable higher at Fensholt (Olesen et al. 2017). The catchment is drained by ca. 9 km of stream network with the outlet at the eastern side. The western and northwestern stream branches drain, respectively, a lowland and forested area (Fig. 1).

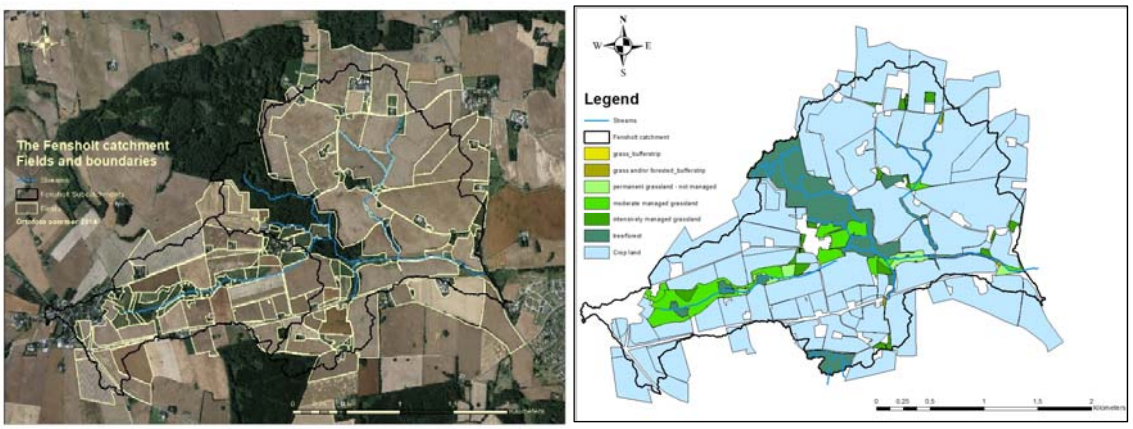


*Figure 1. Left, orthofoto of the Fensholt catchment indicating the agricultural area as fields. Right, cropland map of the catchment showing also grasslands and forest. Apart from streams, other land use classes have been omitted for simplicity.*

The soils in the catchment have primarily developed on till from the Weichsel glaciation and are predominately sandy loams. Luvisols are the most common soil types apart from the western lowland area where Histosols are prevalent. The spatial distribution of soils in the catchment (Fig. 2, left) has been derived from the national soil texture map of Denmark (Adhikari et al., 2013). Overall, the agricultural land in the Fensholt catchment is intensively tile-drained. Therefore, tile drainage can potentially be an important pathway of P loss from agricultural land to surface water. As part of the iDRÆN project and with support from the agricultural advisory service, SEGES, detailed drainage maps have been obtained for the catchment mainly from farmers (Kjærgaard og Iversen, pers. comm.). For some fields, however, no information on the drainage status was available. Based on visual inspections along the stream network and along the boundary between the grassland and the cropland it is be-

lieved that large parts of the unmapped fields actually are drained. This together with interviews with the local farmers suggest that it is likely that the mapped tile-drained area has been underestimated. Fig. 2 (right) shows the extent of the documented tile drainage network. Eighty-four out of 122 fields are at least partly connected to the drainage network. However, the drainage intensity varies markedly both within and between fields. There is no clear spatial pattern, but strongly sloping land and the southern part of the catchment in general appear to be less intensively drained (Fig. 2, right). Given the importance of artificial land drainage for nutrient losses from agricultural land and the difficulty to obtain reliable drainage maps, model-based approaches for predicting the drainage status have been developed. Fig. 2 (right) shows a classification for the Fensholt catchment into drained and non-drained fields based on the model of Møller et al. (2018), which maps the extent of artificially drained areas in Denmark. Accordingly, 83% of the cropland is artificially drained. At a national level, the model had an overall accuracy of 76.5%, and there was generally a reasonable agreement between model prediction and the obtained maps of tile drain networks in the Fensholt catchment. In the context of assessing the risk of P loss in drainage waters, the model results suggest that some of the southern part of the catchment may also be tile-drained. However, field observations in one of the monitored drainage catchments showed that farmer's drainage maps locally may just as well be incorrect and overestimate the extent of tile drainage (Jakobsen et al. 2018). Some areas might not be as systematically drained as the map indicates, and may instead being only point drained by a fewer amount of tile drains less intensively distributed over the fields. Obtaining reliable drainage maps for nutrient loss assessment therefore remains a formidable challenge.

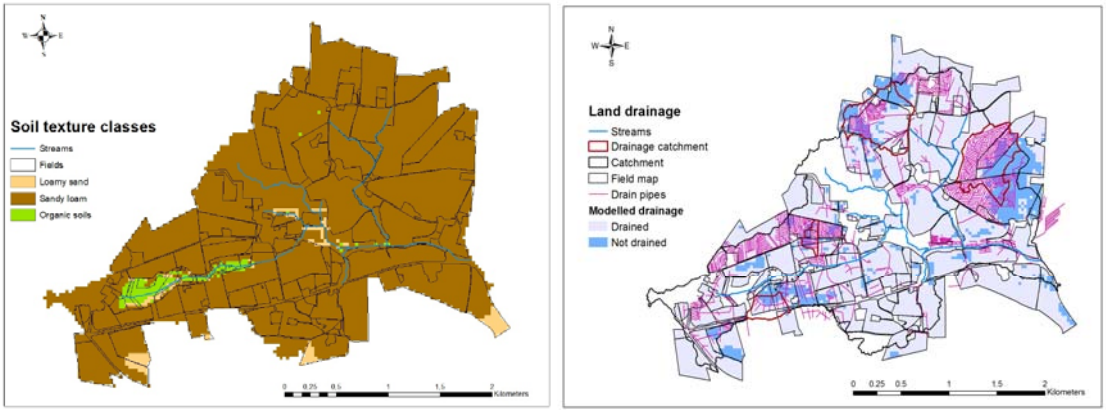


*Figure 2. Left, distribution of soil types in the Fensholt catchment based on the 30-m resolution national texture map of Adhikari et al. (2013). Right, land drainage map of the catchment. Red lines and polygons show the known tile drainage network and the monitored drainage catchments. The blue colours indicate the model-predicted drainage status of agricultural land (Møller et al., 2018).*

The risk of P loss from land to water depends highly on the content of potentially mobile P in soils, which in turn is heavily influenced by the history of P additions with animal manure and mineral fertilizer. Over the past decades, many agricultural soils in Denmark have been enriched with P, especially in areas with intensive animal husbandry in Jutland (Rubæk et al. 2013). With current manure and fertilizer application practices in Denmark, the primary source of P loss is the soil P pool rather than manure or fertilizer P (Andersen et al. 2016).

Nevertheless, information on fertilization practices are valuable for assessing the risk of P loss, because they indicate, whether P accumulation continues at elevated rates. Historical records of P additions to land in the Fensholt catchment are not available. Neither have we information on current P applications rates at the field level. We have therefore used the *FRJOR* database (DJF's *F*orsknings *R*elaterede *JOR*dbrugsregister, FRJOR, 2017) to obtain information on animal manure and fertilizer applications at the farm level for the period 2011-2015. The P content of animal manures was estimated based on standard values in the national *Gødnings- og Husdyrindberetningen* (GHI) database. For spatializing farm-level information on P application the Land Parcel Identification System (LPIS) database and the actual field map of the year 2016 were used. However, farm-average annual P additions on an area basis could not be allocated directly to certain fields, since the ownership of numerous fields as well as their size has varied over the period 2011-2015. Instead, the catchment was divided into a regular 100-m grid and each grid cell received the average annual P input of the associated farm in that year. Finally, this P input information was aggregated for the field map 2016 for presentational purposes (Fig. 3, left).

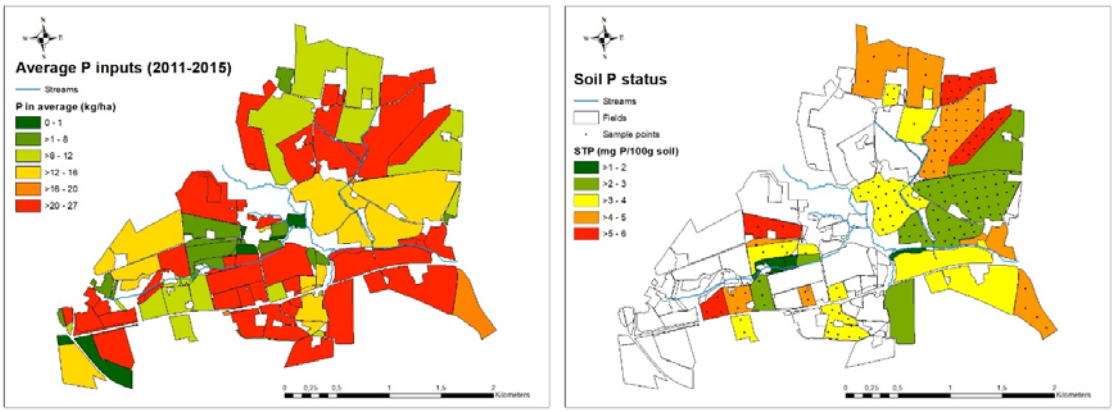


*Figure 3. Left, calculated farm-averaged P inputs to fields (2016 field map) as manure and mineral fertilizer in the Fensholt catchment, annual means for the period 2011-2015. Right, soil P status map of the catchment. Measurements are based on the Olsen P method (Olsen et al., 1954) and have been made during the period 2002-2015. Results are shown as field averages. The colour white represents fields for which we could not obtain data. Dots indicate individual sampling points. Note that sampling points for soil P testing have only been georeferenced in recent years.*

The average annual P inputs to the fields varied between zero and 27 kg P $ha^{-1}$ (Fig. 3, left). In general, these application rates represent moderate P inputs. Thirty-four fields or 175 ha received >20 kg P $ha^{-1}$, and with a typical P offtake by cereal crops of 20 kg P $ha^{-1}$ even the high P input fields are close to P balance. However, individual fields may have received substantially higher P inputs, as the procedure used for estimating annual P inputs averages over a given farm's cropland.

Soil test P values are an expression of the concentration of plant-available P in the plough layer. Plant-available P is primarily loosely bound in soils and exchanges readily with the soil solution. Therefore, it is also closely related to the pool of potentially mobile soil P. In Denmark, soil test P is determined as bicarbonate-extractable soil P according the Olsen P

method (Olsen et al., 1954). Many farmers have their soils tested regularly, typically every fifth year, for Olsen P by certified labs, and the soil sampling is often undertaken by the local farm advisory services. The test results are properties of the farmers, which often are reluctant to release them to third parties. To obtain information on the soil P status, we have with the help of the local farmers' association (LMO) asked all farmers in the Fensholt catchment to provide us with the most recent soil P test results for all fields in the catchment. We acquired data for 36 fields covering 334 ha or 55% of the agricultural area (Fig. 3, right). This illustrates that limited access to soil test P data is a challenge for model-based assessment of the risk of P loss. The quality of the data is variable. The oldest measurements date from 2002, the most recent from 2015. Many fields are represented by a single or just a few soil P test measurements. Often the sample locations are not georeferenced. However, it is common sampling practice for soil testing to bulk several sample from within the same field. It is therefore uncertain, if the inherent spatial variability of soil P is adequately accounted for in all cases by the shown field-averaged soil P test values (Fig. 3, right). Soils with >4 mg Olsen P 100 $g^{-1}$ are considered as having a high soil P status. This was the case for 13 fields of together 134 ha.

# 3 Risk of sediment and phosphorus transfer to water by erosion

The Fensholt catchment is largely characterized by gently rolling topography ranging between 44 m and 101 m elevation AMSL (Fig. 4). Therefore, parts of the catchment may be vulnerable to water erosion, especially in the eastern part where sloping agricultural land borders directly to the stream network. Since P binds strongly to mineral soil particles and is a constituent of soil organic matter, erosion of fertile top soil may not only transfer sediment but also relevant amounts of P to surface waters. The relative P enrichment of eroded sediment with regard to the original soil is widely documented (e.g. Quinton et al. 2001). This is explained by the higher likelihood of long distance transport of fine-textured material, which P preferably binds to. However, enrichment varies spatially and temporally depending on several erosional factors, e.g. erodibility, and soil properties, e.g. clay content and dispersibility. It is therefore a conservative estimate to relate the sediment P concentration directly to the soil P status of eroding areas. Thus, the estimation of sediment delivery by erosion from cropland to water becomes a key component for assessing the risk of P loss to water.

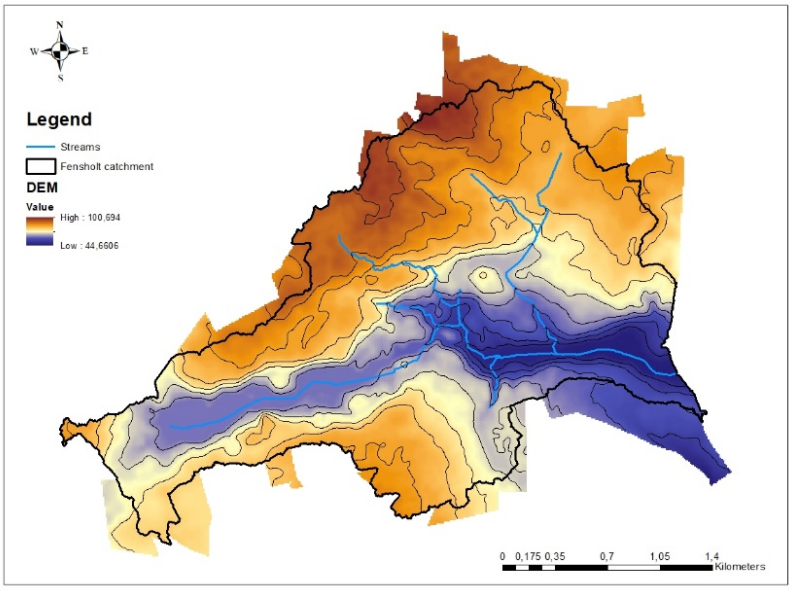


*Figure 4. Digital elevation model (DTM) for the Fensholt catchment. Contour lines are shown for 5 m elevation difference.*

We used the spatially distributed WaTEM tool (Van Oost et al., 2000) to estimate soil redistribution by water in the catchment. The water erosion component in WaTEM is based on RUSLE (Renard et al., 1997) and calculates long-term average annual soil erosion rates:

$$E = R\,K\,L\,S_{2D}\,C \quad (1)$$

where E is the mean annual soil loss (t $ha^{-1}$ $year^{-1}$), R is a rainfall erosivity factor (MJ mm $ha^{-1}$ $hr^{-1}$ $year^{-1}$), K is a soil erodibility factor (t hr $MJ^{-1}$ $mm^{-1}$), $LS_{2D}$ is the unitless two-dimensional slope-length factor accounting for convergent and divergent flow (Desmet and Govers, 1996), and C is a dimensionless crop management factor. The C factor scales the erosion

risk associated with a given crop compared to bare fallow. Input data include long-term rainfall data from weather stations across Denmark typically for the period 1988 to 2012 for estimating the R factor. A national soil texture map (Adhikari et al., 2013) was used to derive the K factor according to Renard et al. (1997). A 10-m resolution digital elevation model (DTM) derived from LiDAR data (Rosenkranz and Frederiksen, 2011) is the input for calculating the $LS_{2D}$ factor (Desmet and Govers, 1996). The C factor is estimated from 10-year crop rotation data from the LPIS database. Additionally, the model used Basemap 2012 (Levin et al., 2012), a 10-m land use raster map of Denmark, to account for land use classes. Importantly, WaTEM also estimates spatially distributed deposition rates. To this end, the basic RUSLE model is expanded with a transport capacity concept assuming that sediment movement is limited by transport capacity of runoff. Hence, WaTEM fully accounts for sediment redistribution in landscapes. A detailed description of the model, the input data and the model calibration is reported by Onnen et al. (2018). WaTEM has been calibrated based on 10-year riverine sediment export data from 31 small catchments in Denmark which did not include Fensholt. The output of WaTEM is i) a 10-m raster map of erosion or deposition rates, ii) a 10-m raster map of sediment delivered to streams for each stream network grid cell and iii) a 10-m raster map showing the contribution of each field to sediment delivery to streams.

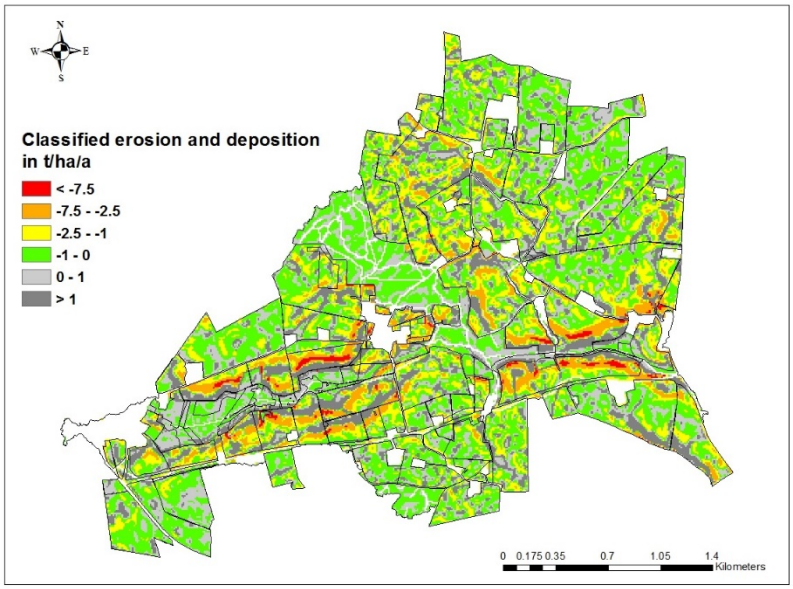


*Figure 5. Modelled annual water erosion and deposition rates aggregated in several classes for the Fensholt catchment. Negative values denote erosion, positive values deposition. Black lines delineate fields.*

The map of classified erosion and deposition (Fig. 5) provides an overview over the soil redistribution in the catchment. Areas of high erosion were predicted on steep slopes bordering the stream valleys. Non-agricultural land has typically low erosion risk or coincides with depositional areas. On the hummocky terrain in the northeast and on the valley floors depositional areas are common. On agricultural land, the majority of soil redistribution rates ranges between 1 t $ha^{-1}$ $year^{-1}$ soil loss and 1 t $ha^{-1}$ $year^{-1}$ deposition (Table 1). This is ranked as tolerable soil loss or deposition (Verheijen et al., 2009). However, about 52 ha or almost 9% of the agricultural area is classified as high erosion risk exceeding 2.5 t erosion $ha^{-1}$ $yr^{-1}$.

*Table 1. Proportion of land area in certain risk classes of water erosion in the Fensholt catchment; 'ero' and 'depo' denote erosion and deposition, respectively.*

| Rates | Potentially erodible land area | | Agricultural land | |
|---|---|---|---|---|
| t ha$^{-1}$ year$^{-1}$ | Area, ha | Area, % | Area, ha | Area, % |
| (ero) > 7.5 | 5.6 | 0.8 | 5.6 | 0.9 |
| (ero) 7.5 - 2.5 | 46.9 | 6.9 | 46.8 | 7.9 |
| (ero) 2.5 - 1 | 119.0 | 17.6 | 118.4 | 20.0 |
| (ero) 1 - 0 | 256.0 | 38.0 | 214.7 | 36.2 |
| (dep) 0 - 1 | 140.1 | 20.8 | 110.0 | 18.6 |
| (dep) > 1 | 107.0 | 15.9 | 96.9 | 16.4 |

Some of the eroded sediment eventually reaches the stream network impacting the aquatic environment. The annual sediment delivery from all land area to streams has been calculated for 10-m grid cells overlapping with surface water and varies between zero and about 350 kg sediment per 10-m grid cell in the catchment (Fig. 6). Sediment delivery is much skewed with a median of only 4 kg sediment per cell. The total estimated sediment delivery to the stream network in the Fensholt catchment amounts to about 26 t sediment year$^{-1}$, some of which may have originated from outside agricultural land. The model output thus enables us to locate likely hotspots of sediment transfer to streams, which is valuable information for targeted mitigation planning.

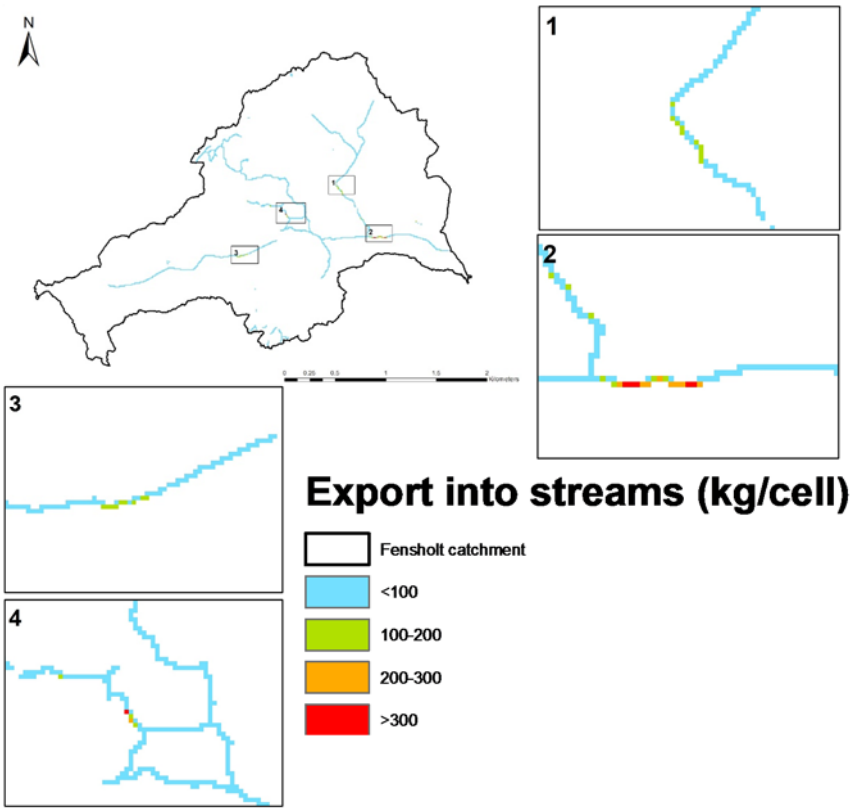


*Figure 6. Modelled sediment delivery to streams in the Fensholt catchment presented as different classes. Sediment delivery is shown as mass for 10-m grid cells that overlap with streams. There are four areas with relatively high sediment delivery shown as insets.*

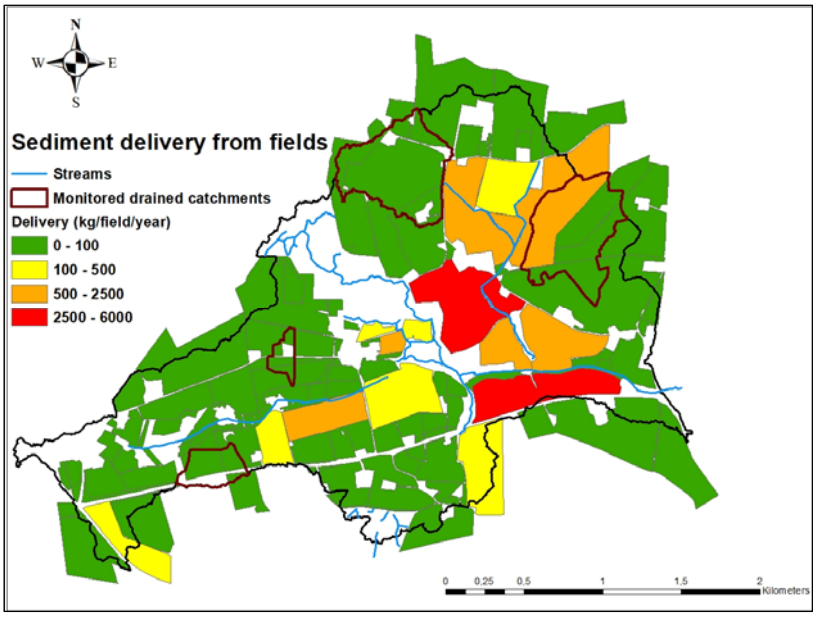


*Figure 7. Aggregated mass of sediment delivered from a given field to streams presented as different classes. Additionally, the four monitored drainage catchments are indicated.*

One way to address P losses is implementing end-of-pipe measures that attempt to capture P in runoff before it enters surface water or even after entering in the form of in-stream sediment traps. Other approaches are directed at the source of P loss and hence agricultural fields including reduced tillage, improved soil cover or crop selection. It is therefore important to estimate how much sediment is lost from individual fields to streams. Fig. 7 shows the predicted risk of aggregated annual sediment loss from individual fields to surface water. Note that fields with relatively high aggregated sediment loss to streams do not necessarily border stream stretches with high rates of sediment delivery (Fig. 6, 7). The overall erosional sediment delivery from agricultural land to water in the Fensholt catchment amounts to 19.3 t year$^{-1}$, and the difference to the total sediment delivery can be attributed to non-agricultural land. Two fields stand out as hot spots with annual deliveries of 3.0 t and 5.4 t of sediment or 43 % of the total. Assuming an average TP concentration of 580 mg P kg$^{-1}$ soil for loamy soils (Rubæk et al., 2013), the annual erosional P load would amount to 1.7 and 3.1 kg P from these fields, respectively. In terms of limiting P transfer from fields to streams, erosion protection measures, e.g. as riparian buffer zone, should to be considered, especially on these fields. The corresponding total annual P delivery to streams in the catchment of 11.2 kg P is rather low.

# 4 Erosion risk scenarios under land use and climate change

## 4.1 Scenarios for changes in cropping systems, land use and climate

The effect of different land use and adapted cropping practices on the risk of soil erosion and sediment delivery to streams is highly dependent on the spatial context in landscapes. Conservation measures that target high-risk areas and the main paths of runoff connectivity in landscapes are typically most effective. Numerous mitigation measures for reducing erosion risk and its consequences are well known and widely used. They range from agronomic measures like reduced tillage or direct drilling to the establishment of buffer zones for sediment retention (Govers et al. 2004). The present analysis assesses the effect of land use and crop system scenarios SSP1 and SSP5 (Olesen et al., 2017) under a wetter climate in the Fensholt catchment for the 2040-2060 period under the RCP8.5 emission scenario. The scenarios have been spatialized based on simple assumptions. To this end, the SSP1 and SSP5 scenarios have been adapted to a minor extent in accordance with erosion modelling premises (Table 2).

*Table 2. Overview of erosion modelling scenarios. Land use scenarios and corresponding crop rotations for pig and dairy farms were adapted from Olesen et al. (2017) in accordance with erosion modelling premises.*

| Land use demand | Transition rules | Scenario | C factor on cropland |
|---|---|---|---|
| 11% reduction in agricultural land by establishing 60 m wide riparian buffer zones on both sides of streams. Equal proportion of pig and dairy farm cropland. | Conversion to grassland | SSP1.1 | C factor from national erosion modelling (Onnen et al. 2018), average 0.33 |
| | | SSP1.2 | Common C factor 0.255 assuming equal distribution of pig and dairy farm crop rotations. In the long-term all cropland is equally used by pig and dairy farms. |
| | | SSP1.3 | Dairy farm crop rotations on half of the cropland closest to streams corresponding to fields within a 220-m zone on both sides of streams, C factor 0.22. Remaining cropland with pig farm crop rotations, C factor 0.29. |
| 7% increase in cropland. Equal proportion of pig and dairy farm cropland. | Conversion from grassland and forest | SSP5.1 | C factor from national erosion modelling (Onnen et al. 2018), average 0.33, which also is allocated to converted land. |
| | | SSP5.2 | Common C factor 0.27 assuming equal distribution of pig and dairy farm crop rotations. In the long-term all cropland is equally used by pig and dairy farms. |
| | | SSP5.3 | Pig farm crop rotations on half of the cropland closest to streams corresponding to fields within a 220-m zone on both sides of streams, C factor 0.33. Remaining cropland with dairy farm crop rotations, C factor 0.21. |

Changes in crop management are expressed via the C factor in the RUSLE model (Eq. 1). Since specific crop management factors for cropping practices in Denmark are not available, we have assigned typical C factors from the literature (Morgan, 2005; Panagos et al. 2015) to individual crops in rotations of scenarios SSP1 and SSP5 (Olesen et al. 2017; Table 4.1). Table 3 shows the averaged C factors for the corresponding pig and dairy farm crop rotations assuming that all elements of the rotations are grown in equal proportions.

For the SSP1 and SSP5 scenarios, we have assessed soil redistribution in the Fensholt catchment for three specific combinations of land use change and crop rotations (Table 2), which we refer to as erosion scenarios. The SSP1 scenarios assess in general ca. 10% reduction in cropland (Olesen et al. 2017). This has been accounted for in erosion modelling by establishing 60-m wide riparian buffer zones on formerly arable land along the stream network. Those buffer zones were considered covered by grassland and amounted to 50 ha or 11% of the original cropland in the Fensholt catchment. The SSP1.1 erosion scenario (Table 2) uses the spatial C factor distribution from the national soil erosion modelling (Onnen et al., 2018). The C factors are based on area-weighted cropping information that was taken from the LPIS database for the period 2005-2014 and aggregated on a 1-km$^2$ grid. The SSP1.2 erosion scenario assumes an equal distribution of farmland between dairy and pig farms and hence a substantial reduction in pig production. This results in a lower C factor. In the long term, the crops associated with the two farm types (Table 4.1, Olesen et al. 2018) are grown equally on all fields resulting in an average C factor for all arable land (Table 2). In the SSP1.3 erosion scenario the arable land is still equally divided between pig and dairy farms; however, all land of dairy farms is located near surface water, while the cropland of pig farms is located in a belt around the dairy cropland. Thus, cropland closer to streams has a lower C factor. Practically, dairy farms had 199 ha cropland in a 220-m zone on each side of the streams in the catchment compared to 204 ha cropland of pig farms. The different C factors in the two zones reflect the different crop rotations (Table 2).

*Table 3. Average annual crop management factors, C factors, assigned to crop rotations of the SSP1 and SSP5 scenarios (Olesen et al. 2017). Typical C factors for individual crops were taken from the literature.*

| Farm type | SSP1 | SSP5 |
|---|---|---|
| Pig/plant | 0.29 | 0.33 |
| Dairy | 0.22 | 0.21 |

In the SSP5 scenarios, we consider an increase in the cultivated area by converting grassland and forest in the catchment to cropland (Table 2). Practically all grassland registered in the land use map (Basemap) was converted. Additionally, forest was converted when it bordered on cropland and had a terrain slope <6 degrees amounting to 5 ha in all. The total converted land area comprised 31 ha or 7% of the original cropland in the catchment and, therefore, fell slightly short of the 10% target. The SSP5.1 erosion scenario (Table 2) uses again the spatial C factor distribution from the national soil erosion modelling (Onnen et al., 2018). The average C factor for the catchment is allocated to the converted areas. The SSP5.2 erosion scenario assumes an equal distribution of farmland between dairy and pig farms. Due to different crop rotations, the average C factor is higher than for SSP1.2 (Table

2). Finally, in the SSP5.3 erosion scenario the location of cropland of pig and dairy farms is reversed compared to SSP1.3 as part of a worst-case assumption. Arable land is still equally divided between pig and dairy farms, however, all land of pig farms is located near surface water, while the cropland of dairy farms is located in a belt around the dairy farmland. Thus, cropland closer to streams has a higher C factor (Table 2).

Erosion risk was assessed for the six land use change and cropping scenarios (Table 2) both with the annual rainfall erosivity, R factor, of the national erosion modelling (Onnen et al. 2018) and a 20% increased annual rainfall erosivity in accordance with the climate change scenarios of Olesen et al. (2017, Table 4.9). The former will be referred to as present rainfall erosivity. This resulted in 12 erosion risk scenarios in total. Given the basic structure of the erosion model (Eq. 1), an increase in rainfall erosivity will directly increase erosion risk in parts of the landscape. However, the effect on spatial patterns of soil mobilization and deposition will highly depend on topography.

## 4.2 Erosion risk scenario results

Under present rainfall conditions, the SSP1 scenarios show a reduction of the area with high (>7.5 t $ha^{-1}$ $yr^{-1}$) or moderately high (2.5-7.5 t $ha^{-1}$ $yr^{-1}$) erosion risk on cropland in the Fensholt catchment (Fig. 8) compared to the national erosion model setup (baseline erosion). In relative terms, the high erosion risk areas are more strongly affected. This is partly due to the reduction in cropland. However, the lower C factors in SSP12 and SSP13 of the adapted crop rotations (Table 2) are relatively more important and contribute to reducing the high-erosion risk area to, respectively, 34% and 21% of the extent associated with the baseline erosion. The corresponding reduction effects of the area with moderately high erosion were 60% and 57%.

By increasing the annual rainfall erosivity by 20% in SSP1, the areas with high and moderately high erosion risk increase expectedly in all cases compared to present rainfall erosivity (Fig. 8). For SSP12 and SSP13 the high-erosion risk area doubles. However, only in SSP1.1 the area with high and moderately high erosion risk is larger than for the national erosion modelling setup (Fig. 8). Here higher rainfall erosivity overcompensated for the reduction in cropland by 11% in the catchment. The lower cropping factors in SSP1.2 and SSP1.3 result in high-erosion risk areas that are only 68% and 50% of the size under the baseline erosion scenario. The corresponding reduction effects for the area with moderately high erosion were 76% and 73% (Fig. 8).

In SSP5 (Table 2), which represents 7% more cropland in the Fensholt catchment than the national erosion model setup, the high-erosion risk area increases for SSP5.1 and SSP5.3 assuming present rainfall erosivity (Fig. 8). The effect is larger than the increase in cropland suggesting that the new farmland is particularly erosion vulnerable. Despite a lower C factor on dairy farm land distal to the stream network in the latter scenario (Table 2), the similar size of the high-erosion risk area in SSP5.1 and SSP5.3 indicates that high-erosion risk topography is located closer to streams. Only the SSP5.2 scenario has a 19% lower area with

high erosion risk due to an overall lower cropping factor compared to the other two scenarios (Table 2). The SSP5 scenario effects are less pronounced for the size of the moderately high erosion risk area (Fig. 8). A 20% increase in rainfall erosivity leads to a doubling of the high-erosion risk area, while the effect on the area with moderately high erosion risk is rather low (Fig. 8). This illustrates that climate change effects, such as increased rainfall erosivity, exacerbates the erosion problem on the most vulnerable areas.

The scenario analyses show that adapted cropping practices are key to reducing the impact of higher rainfall erosivities under climate change on soil erosion. Importantly, this ought to be a manageable task for farmers, as more sustainable crop rotations under SSP1 are not radically different from current ones.

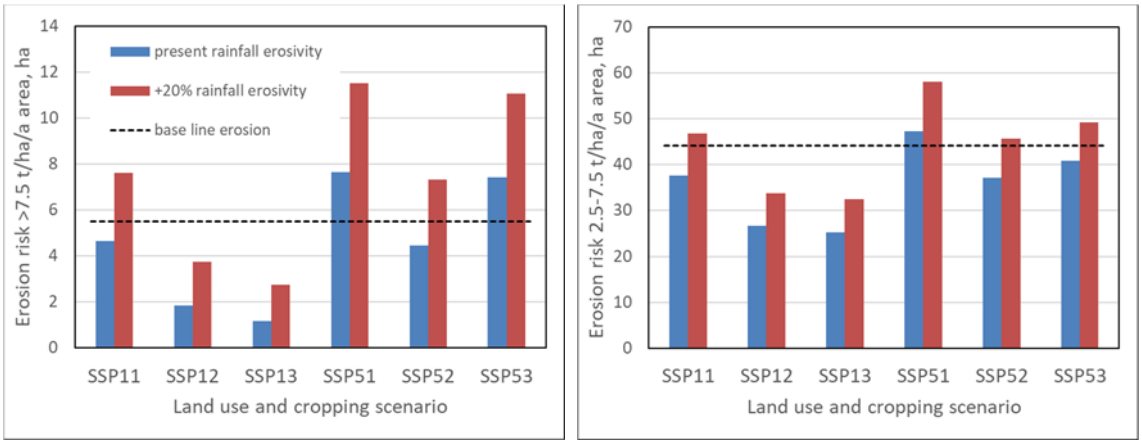


*Figure 8. Model-predicted total area within a certain erosion risk class (Table 1) for six land use and cropping scenarios as well as two climate scenarios in the Fensholt catchment. Left, area with high erosion rates of >7.5 t ha$^{-1}$ yr$^{-1}$. Right, area with moderately high erosion rates between 2.5 and 7.5 t ha$^{-1}$ yr$^{-1}$. The scenarios are described in Table 2. Present rainfall erosivity has been estimated for the period 1988-2012. The dashed lines indicate the corresponding area for the respective risk class estimated by the national erosion model setup.*

The spatial extent of eroding areas is only one of several criteria for assessing sustainable land management. The transfer of nutrient-rich sediment from agricultural land to water is another. Fig. 9 summarizes the predicted total annual sediment delivery into streams for all land use and crop rotation scenarios as well as for the two climate scenarios in the Fensholt catchment. The SSP1 scenarios reduce sediment delivery by more than 70% and differ only marginally from each other. The increase in rainfall erosivity has little effect for these scenarios. The effects are overwhelmingly the result of converting cropland into wide riparian buffer zones covered by grass (Table 2). Riparian buffer zones are known to retain eroded sediment effectively (e.g. Hickey and Doran, 2004). In our case, they limit the amount of sediment reaching the water system by about 20 t yr$^{-1}$ (Fig. 9).

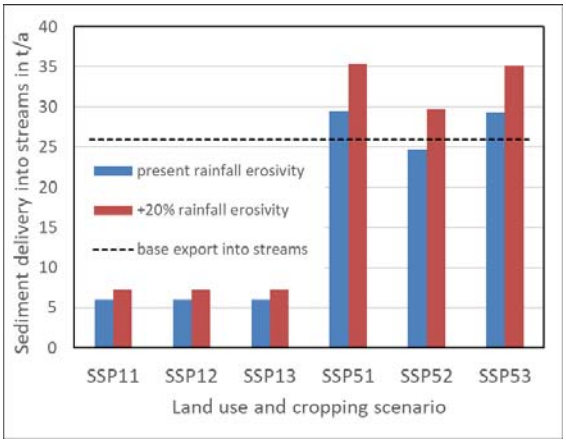


*Figure 9. Model-predicted total annual sediment delivery into streams for six land use and cropping scenarios as well as two climate scenarios in the Fensholt catchment. The scenarios are described in Table 2. Present rainfall erosivity has been estimated for the period 1988 -2012. The dashed line indicates the amount of sediment delivery estimated by the national erosion model setup.*

Without extensive areas of riparian buffer zones, sediment delivery to streams in the SSP5 scenarios is typically larger compared to the national erosion model setup (Fig. 9). Converting 7% of the cropland to grassland and forest alone (SSP5.1, Table 2) results in a 14% increase in sediment delivery. A similar increase is observed in SSP5.3 despite a substantially lower C factor on cropland distal to the streams (Fig. 9). This indicates that cropland closer to streams is the predominant source for sediment delivery. The lower sediment delivery of SSP5.2 with present rainfall erosivity is due to the overall lower C factor in this scenario (Table 2). A 20% increase of rainfall erosivity induces higher sediment delivery for all SSP5 scenarios (Fig. 9). The ranking of the three SSP5 scenarios is the same for both rainfall erosivities. For scenarios SSP51 and SSP5.2 sediment delivery rises by about 35%. Hence, the relative effect on sediment delivery is markedly larger than the increase in rainfall erosivity.

In general, changes in cropping practices and climate do not affect the erosion risk area and the sediment delivery to streams proportionally. Our scenario analyses illustrate the importance of buffer zones for breaking the hydrological connectivity of surface runoff and retaining sediment in landscapes. However, these scenarios work with simplified assumptions of, amongst others, land use change to facilitate comparisons. Practically, only a small proportion of the modelled riparian buffer zones contributes effectively to sediment retention.

# 5 Phosphorus loss in drainage and streams

As part of the iDRÆN project, a number of tile drainage catchment have been identified in the Fensholt catchment and instrumented with electromagnetic flowmeters at the outlet for recording discharge continuously. Additionally, continuous discharge recordings were made at two stream stations by means of a water level logger (S1 and S2 in Fig. 10). Four of the drainage catchment were subsequently selected for monitoring drainage water quality and are referred to as D1, D2, D7 and D8 (Fig. 10). At each outlet of the drainage catchments and at the stream stations, drainage or stream water samples have been collected automatically and time-proportionally by ISCO samplers. Samples were abstracted hourly and bulked for each day. Amongst other parameters, total P (TP) and turbidity, normalized turbidity units (NTU), were measured in the lab. The ISCO samplers at the drainage catchments were installed as part of the BONUS SOILS2SEA project. The analyses of water samples were mainly financed by other projects including iDRÆN (Kjærgaard and Iversen, 2018, unpublished data). Climate data have been recorded by a weather station near the Fensholt catchment, at Fillerup. Monitoring of discharge commenced in 2012, while a consistent set of water quality data from the six monitoring stations is only available for the period May 2015 to May 2017. Therefore, in the following some data are presented for the runoff season May to May 2015/16 and 2016/17.

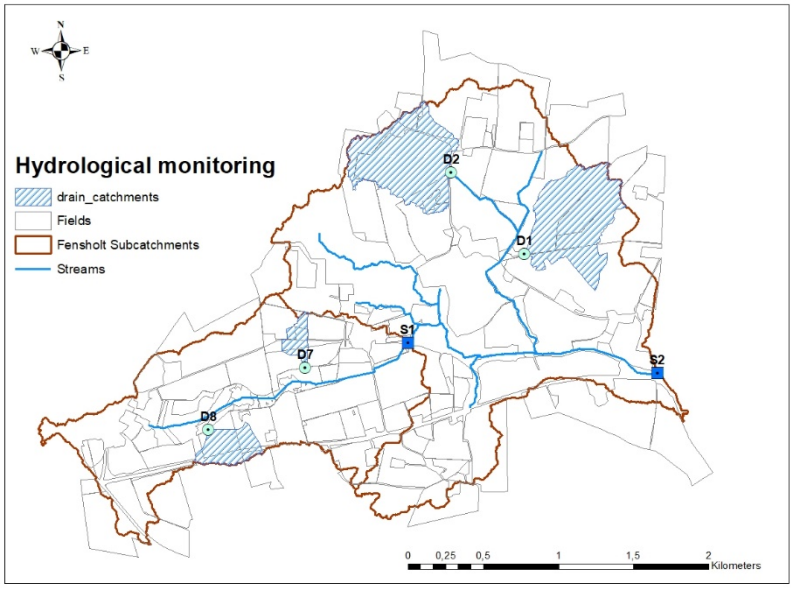


*Figure 10. Map of monitored drainage catchments in the Fensholt catchment indicating also drainage (D1, D2, D7, D8) and stream (S1, S2) monitoring stations.*

The annual precipitation was 1150 and 870 mm in the monitoring periods 2015/16 and 2016/17, respectively. This compares to an average annual precipitation of 870 mm during the period 1990-2015. Fig. 11 shows as an example the daily rainfall and the discharge at the stream station of the catchment outlet and one drainage station. The hydrographs are characterized by peak flow events, and most discharge occurred during the period October to March (Fig. 11).

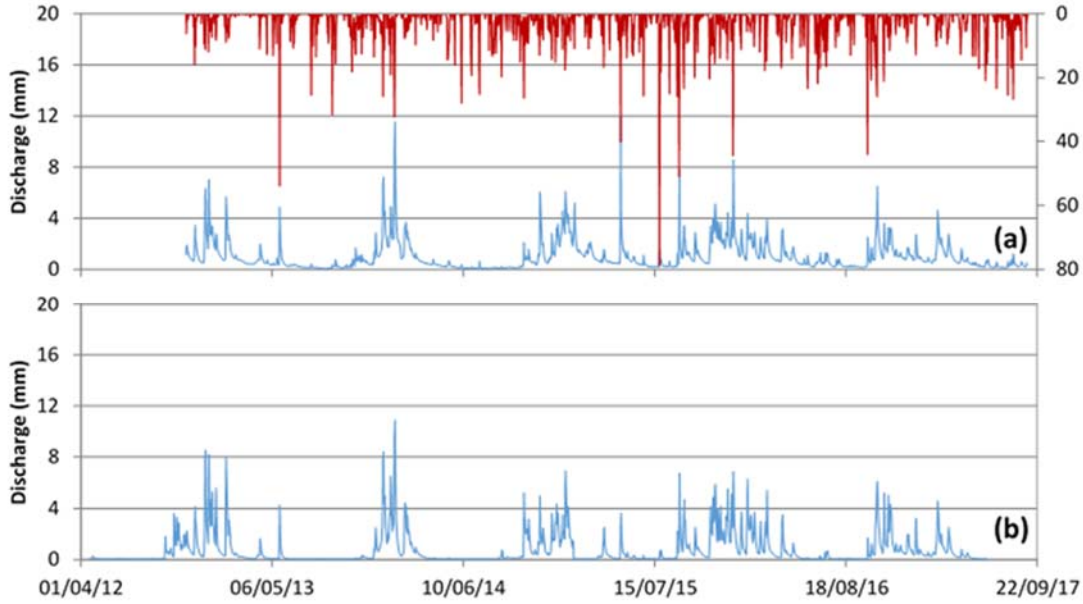


*Figure 11. Daily discharge (blue) for the measuring station in (a) Snærrildvej (S2) and (b) drainage station D1.* Values of precipitation corrected for wind effect according to Allerup og Madsen (1979) *in mm (red) are also shown (Kjærgaard and Iversen, 2018, unpublished data).*

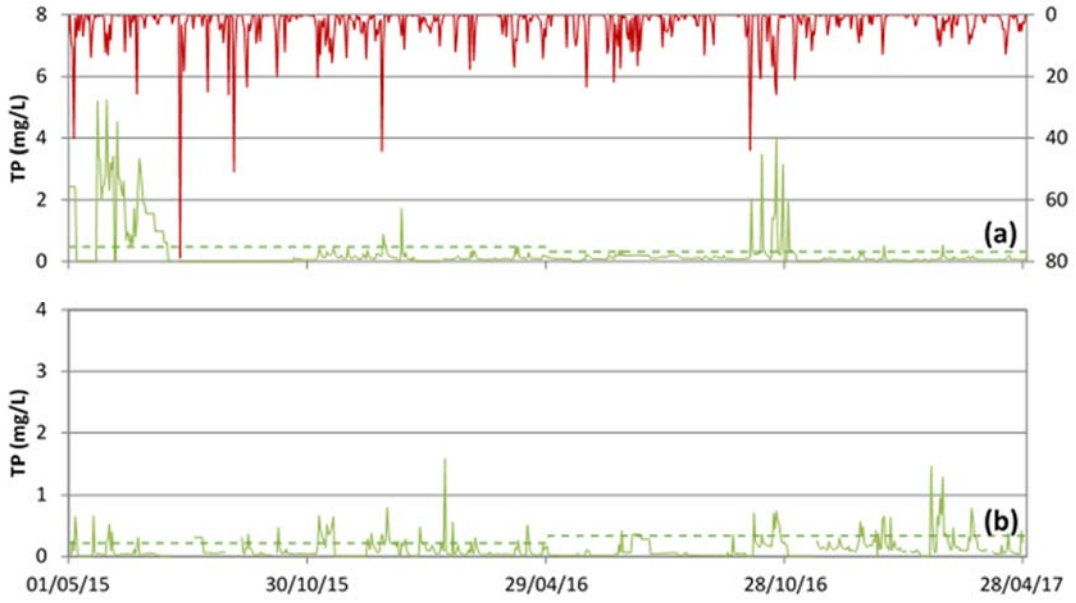


*Figure 12. Examples of daily total phosphorus (TP) concentration (green) for the stream station at (a) Snærrildvej (S2) and (b) the drainage station, D1, between 01/05/2015 and 30/04/2017. The flow weighted average P concentration (dotted line) and the corrected values of precipitation in mm (red) are also shown (Kjærgaard and Iversen, 2018, unpublished data).*

Both in drainage and in stream waters, TP concentrations were temporally highly variable with intermittent peaks (Fig. 12). This is often observed especially for sites with elevated P losses (Andersen et al. 2016). At the catchment outlet, TP concentrations in stream water were sometimes very high and often exceeding 1 mg TP $l^{-1}$. Total P concentrations in drainage were temporarily also high and often exceeded 0.5 mg TP $l^{-1}$ (Fig. 12). There was no clear temporal trend for the occurrence of peak TP concentrations, in neither drainage nor stream waters.

Phosphorus is lost in runoff both in dissolved and particulate form. When water movement in soils occurs as macropore flow, P-enriched colloidal material can be rapidly transported from the top soil to tile drains. Under such conditions, particulate P makes a substantial contribution to total P losses, which then are often much higher than under matric flow conditions (e.g. de Jonge et al. 2004). The sandy loam soils of the Fensholt catchment have a moderate to high susceptibility for macropore transport (Iversen et al. 2011). Also in stream runoff, particulate P can make an important contribution to the TP load. This particulate material originates from different erosional processes including stream channel erosion as well as drainage waters. Due to resource limitations, we did not determine particulate P nor suspended sediment in runoff. Instead, we have used the turbidity NTU measurements as a surrogate for suspended sediment. Both in stream and in drainage waters there was a close positive correlation between TP and NTU (Fig. 13), indicating an important contribution of particulate P to TP. This is consistent with previous findings of runoff composition from loamy catchments (e.g. Kronvang et al., 1997; Andersen et al., 2016) and the likely occurrence of macropore transport.

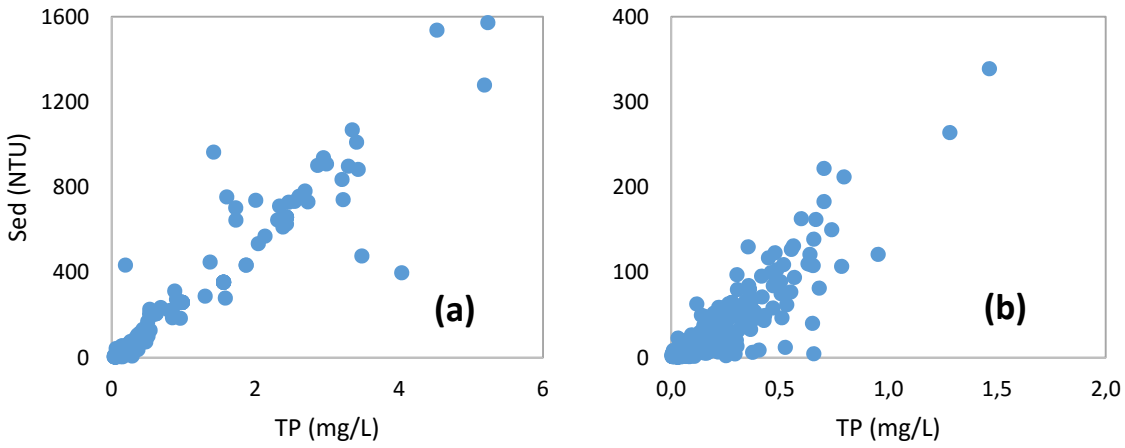


*Figure 13. Sediment concentration expressed as NTU versus daily TP concentration. Examples are shown for (a) stream water, Snærrildvej (S2), and (b) drainage water (D1) during the period 01/05/2015 and 30/04/2017 (Kjærgaard and Iversen, 2018, unpublished data). Note the different axes' scales.*

Table 4 summarizes the discharge, rainfall and the TP losses at six monitoring stations in the Fensholt catchment for two consecutive 12-months monitoring seasons. The ratio of discharge to rainfall (Q/P) varied between 0.30 and 0.48 at the four drainage stations in the runoff season 2015/16 and 0.16 and 0.51 in the season 2016/17. This corresponds to Q/P

ratios of other drainage catchments in Weichsel moraine landscapes of Jutland (B.V. Iversen, pers. comm.). In the intensively tile-drained Fensholt catchment, these Q/P ratios indicate that a substantial proportion of rainfall was drained via near-surface runoff (i.e. surface runoff and drainage) from the catchment. The wider range and the generally lower values in the runoff season 2016/17 are broadly explained by lower rainfall compared to the previous run-off season. In general, several factors influence variations between drainage catchments, including local geological variation, the position of the drainage catchment on the hydro-topographic sequence, crops and not least uncertainty about the exact extent of the drainage catchment.

*Table 4. Catchment area, total discharge (Q), ratio between Q and corrected precipitation (P), TP load, flow-weighted average TP concentration and sediment loads for two hydrological years, May to May 2015/16 and 2016/17, at drainage stations D1, D2, D7, D8, and stream stations Snærrildvej (S2) and Skovlyvej (S1) in the Fensholt catchment (Kjærgaard and Iversen, 2018, unpublished data).*

| Measuring station | | D1 | D2 | D7 | D8 | S2 | S1 |
|---|---|---|---|---|---|---|---|
| Catchment area (ha) | | 33 | 33 | 3.7 | 8.4 | 606 | 194 |
| May 2015/16 | Q (mm) | 409 | 545 | 558 | 349 | 511 | 394 |
| | Q/P (-) | 0.36 | 0.47 | 0.48 | 0.30 | 0.44 | 0.34 |
| | TP (kg/ha) | 0.9 | 1.3 | 1.1 | 1.1 | 2.4 | 1.1 |
| | Flow weighted average TP (mg/L) | 0.22 | 0.24 | 0.20 | 0.32 | 0.47 | 0.28 |
| May 2016/17 | Q (mm) | 240 | 446 | 139 | 246 | 346 | 291 |
| | Q/P (-) | 0.28 | 0.51 | 0.16 | 0.28 | 0.40 | 0.33 |
| | TP (kg/ha) | 0.8 | 0.9 | 0.2 | 0.3 | 1.1 | 0.8 |
| | Flow weighted average TP (mg/L) | 0.34 | 0.22 | 0.17 | 0.13 | 0.32 | 0.26 |

In general, the flow-weighted average TP concentrations were high, both in drainage and stream waters of the Fensholt catchment (Table 4). Total P concentrations measured in the stream at the catchment outlet during the two years were about twice or thrice higher than long-term average (1981-2010) TP concentrations predicted by the E-HYPE hydrological and nutrient transport model (Bartosova et al. 2018) for the whole of the Norsminde catchment, of which Fensholt is a subcatchment. We presently lack information for explaining the discrepancy. In high P loss loamy drainage catchments in Denmark, long-term average flow-weighted TP concentrations ranged between 0.08 and 0.18 mg TP $l^{-1}$ (Blicher-Mathiessen et al., 2015). On average in Denmark, stream discharge to the sea had rather stable P concentrations of about 0.13 mg TP $l^{-1}$ during the period 2010-2014 that could be related to diffuse, mainly agricultural sources (Jensen et al., 2015). Hence, at the outlet of the Fensholt catchment TP concentration were about four times higher than on average in Denmark. The importance of point sources for the P loss from the Fensholt catchment is not known. However,

since TP concentrations in drainage and stream waters roughly agree, it is unlikely that point sources make a substantial contribution. During the high rainfall, high discharge season of 2015/16 TP concentrations tended to be higher, especially in stream water at the catchment outlet, indicating discharge-induced higher erosion and transport of particulate P.

Total P loads in the Fensholt catchment were high varying between 1.1 and 2.4 kg TP $ha^{-1}$ at the catchment outlet (Table 4). The average annual P load from agricultural land in Denmark to the sea currently is estimated to be about 0.5 kg TP $ha^{-1}$ (Andersen et al., 2016). Likewise, the E-HYPE modelled TP loads for the Norsminde catchment (Bartosova et al. 2018) were substantially lower than the measured loads at Fensholt (Table 4). This difference is mainly explained by the low, modelled TP concentration in stream discharge for the Norsminde catchment, as the predicted long-term annual discharge for the Norsminde catchments falls well within the stream discharge measurements of the Fensholt catchment (Table 4; Bartosova et al. 2018). Similarly, TP loads from the Fensholt drainage catchments, especially D1 and D2, clearly exceeded those from other loamy drainage catchments in Denmark. The maximum TP loads reported for a 15-year monitoring programme of two high-loss catchments were 0.25 and 0.55 kg TP $ha^{-1}$ (Blicher-Mathiesen et al. 2015). The role of the source factors for TP losses in drainage in the Fensholt catchment was difficult to ascertain. The soil P status was relatively high in the drainage catchments D7 and D8, while it was mainly low in D2 and unknown in D1. However, there was a relatively close relationship between the annual discharges and the TP loads of all stations consistent with other studies (Andersen et al. 2016). Therefore, it would be highly valuable for the risk assessment of P loss in drainage waters, if robust methods for predicting the amount of drainage discharge based on mapped soil, crop and climate data could be developed (Iversen et al. 2016). It was not possible to identify a deterministic model that could be set-up and parameterized for the Fensholt catchment at the fine spatial scale necessary to account for variations of P loss from different fields under different land use and climate scenarios.

*Table 5. Scenarios of sources to the total P load at the outlet of the Fensholt catchment. Catchment loads are calculated based on Table 4, where the seasons 2015/16 and 2016/17 are considered high and low discharge, respectively. Eighty percent of the cropland is assumed tile-drained. The contribution of stream bank erosion has been estimated based on Kronvang et al. (2012) ranging between 25% and 50%. The contribution of soil erosion has been derived from the erosion modeling exercise.*

| Source | High discharge 2015/16 | Low discharge 2016/17 |
|---|---|---|
| | kg TP $yr^{-1}$ | |
| Total load, catchment | 1454 | 533 |
| Drained cropland, min - max | 324 - 468 | 72 - 324 |
| Stream bank erosion | 364 - 727 | 133 - 267 |
| Soil erosion | 15 | 15 |

In the Fensholt catchment, the contribution of tile drainage to the total P load far exceeds that of soil erosion according to our analyses (Table 5). Another important component of the P load in streams is stream bank erosion. Kronvang et al. (2012) found that the process

accounted for about 20 to 60% of the diffuse P losses in the river Odense catchment during three years. For comparing the importance of different sources to the total P load in the Fensholt catchment, we estimate the minimum and maximum contribution of stream bank erosion to range between 25% and 50% (Table 5). A large contribution is consistent with the mobilization of P-enriched soils in stream banks that previously may have been deposited there by soil erosion processes. During the year with low discharge, the contributions from the three transport processes can account for the total catchment P load assuming rather maximum contributions from both tile drainage and stream bank erosion. During the year with high discharge or with lower contributions from tile drainage and stream bank erosion, there remain sizable discrepancies compared to the catchment P load (Table 5). The contribution of other sources, like sewage or scattered dwellings, to the total P load are not known for the Fensholt catchment. Since the catchment is sparsely populated, we expect that the P load derives largely from diffuse sources. Considering that P losses in drainage are generally high in the catchment, it is therefore likely, that the contribution from surface runoff processes has been underestimated. The estimated small P delivery to streams by soil erosion accounts for neither P enrichment in eroded sediment nor the P input in dissolved or colloidal form by surface runoff.

# 6 Conclusions

Phosphorus losses from agricultural land to surface waters pose a threat to the aquatic environment, and to achieve environmental targets, agricultural P losses have to be reduced markedly. P-losses to stream water can follow three main routes: 1) surface erosion, 2) subsurface drainage, and 3) stream bank erosion. Measurements and modelling was conducted for the Fensholt catchment in Denmark to quantify these different components. Measurements over two runoff seasons showed annual total P (TP) loads at the catchment outlet of 1.1 to 2.4 kg TP $ha^{-1}$. This is higher than the estimated average annual P load of 0.5 kg TP $ha^{-1}$ for agricultural land in Denmark and similarly lower than the modelled TP load using the E-HYPE model. The TP in drainage water was found to contribute to about half of the TP in the stream with 0.2-0.9 and 0.9-1.3 kg TP $ha^{-1}$ in the two respective runoff seasons, depending on drainage station. Model-based estimates of stream bank erosion suggested that this contributed between 25-50% of the TP load. Modelling of surface erosion suggest that this was by far the smallest contribution, although this may have been underestimated, given the high contributions from drainage.

The projected climate change for 2040-2060 under RCP8.5 indicate higher rainfall intensity, which is translated into a 20% increase in erosivity. This enhanced the area at risk of high soil erosion by ca. 30-100%, depending on agricultural cropping practices. The increase in area of moderate erosion risk was smaller, ca. 20%. The soil erosion was further substantially affected by land use change, where establishing 60 m wide riparian buffer zones reduced delivery of sediments (and P) to streams to 20% of the baseline load. In contrast, the expansion of agricultural land had very little effect on sediment load to the streams. However, the erosion was only a minor part of the total P load from this catchment, and therefore the overall effects will be small. However, it may be expected that similar effects of climate change though rainfall intensity will be seen on P transported through drains and possibly from stream bank erosion.

This study points to a range of uncertainties in quantifying P losses as affected by climate change and land use change. First, it was not possible to obtained detailed maps of the soil P status in the catchment, and the large contribution of TP from drainage suggests that at least some parts of the agricultural fields have high soil P status contributing to this loading. This points to the need for improved spatial mapping of risk areas for P losses, also when evaluating how this may be affected by climate change and to better target spatially differentiated measures for reducing P losses. Such measures need not only to target critical source areas, but also loss pathways, e.g. surface erosion or subsurface drainage systems.

# 7 References

Adhikari, K., Kheir, R. B., Greve, M. B., Bøcher, P. K., Malone, B. P., Minasny, B., McBratney, A. B. and Greve, M. H., 2013. High-resolution 3-D mapping of soil texture in Denmark. Soil Science Society of America Journal 77, 860-876.

Allerup, P., Madsen, H. (1979) Accuracy of point precipitation measurements. Klimatologiske Meddelelser, no. 5, Danmarks Meteorologiske Institut.

Andersen, H.E., Baatrup-Pedersen, A., Blicher-Mathiessen, G. et al. 2016. Redegørelse for udvikling i landbrugets fosforforbrug, tab og påvirkning af vandmiljøet. Teknisk rapport fra DCE - Nationalt Center for Miljø og Energi nr. 77.

Bartosova, A. et al. 2018. Water Quality Changes in the Baltic Sea basin within the HYPE modelling framework. BONUS Soils2Sea Deliverable 5.1. Swedish Meteorological and Hydrological Institute, Norrköping, May 2018. www.Soils2Sea.eu

Blicher-Mathiessen, G., Rasmussen, A., Rolighed, J. et al. 2015. LANDOVERVÅGNINGS-OPLANDE 2014. Novana. Videnskabelig rapport fra DCE – Nationalt Center for Miljø og Energi nr. 164.

de Jonge, L.W., Møldrup, P., Rubæk, G., Schelde, K., Djurhuus, J. 2004. Particle leaching and particle-facilitated transport of phosphorus at field scale. Vadose Zone Journal 3, 462-470.

De Schepper, D., Therrien, R., Refsgaard, J.C., He, X., Kjaergaard, C., Iversen, B.V. 2017. Simulating seasonal variations of tile drainage discharge in an agricultural catchment. Water Resources Research 53, 3896-3920.

Desmet, P.J.J. and Govers, G., 1996: A GIS procedure for automatically calculating the USLE LS factor on topographically complex landscape units. Journal of Soil and Water Conservation 51, 427–433.

Govers G., Poesen J., Goosens D. 2004. Soil erosion — processes, damages and counter measures. In: Schjønning P, Elmholt S, Christensen BT, editors. Managing soil quality. Challenges in modern agriculture. Wallingford, UK: CABI Publishing. p. 199–217.

Heathwaite, A.L., Dils, R.M. 2000. Characterising phosphorus loss in surface and subsurface hydrological pathways. Science of the Total Environment 251, 523-538.

Hickey, M.B.C., Doran, B., 2004. A review of the efficiency of buffer strips for the maintenance and enhancement of riparian ecosystems. Water Quality Research Journal of Canada 39, 311-317.

Iversen, B.V., Børgesen, C.D., Lægdsmand, M., Greve, M.H., Heckrath, G., Kjærgaard, C. 2011. Risk predicting of macropore flow using pedotransfer functions, textural maps and modeling. Vadose Zone Journal 10, 1185-1195.

Iversen, B.V., Kjærgaard, C., Petersen, R.J., Christensen, S., Rasmussen, K. 2016. Predicting tile drainage discharge. ASA, CSSA, SSSA 2016 Annual Meeting - Phoenix, Arizona, USA.

Jakobsen R., Hansen A.L., Wachniew P., Bar-Michalczyk D., Michalczyk T., Zięba D., 2018. Hill slope studies in Fensholt, Norsminde, Denmark and Kocinka, Poland. Biogeochemical processes and flow paths. BONUS Soils2Sea Deliverable 3.4. Geological Survey of Denmark and Greenland, Copenhagen, February 2018, www.Soils2Sea.eu

Jensen, P.N., Boutrup, S., Fredshavn, J.R., et al. 2015. Vandmiljø og Natur. NOVANA. Videnskabelig rapport fra DCE - Nationalt Center for Miljø og Energi nr. 126.

King, K.W., Williams, M.R., Macrae, M.L., Fausey, N.R., Frankenberger, J., Smith, D., Kleinman, P.J.A., Brown, L. 2015. Phosphorus Transport in Agricultural Subsurface Drainage: A Review. J. Environ. Quality 44, 467-485.

Kronvang, B., Laubel, A., Grant, R. 1997. Suspended sediment and particulate phosphorus transport and delivery pathways in an arable catchment, Gelbæk stream, Denmark. Hydrological Processes 11, 27-642.

Kronvang, B., Rubæk, G., Heckrath, G. 2009. International Phosphorus Workshop: Diffuse Phosphorus Loss to Surface Water Bodies—Risk Assessment, Mitigation Options, and Ecological Effects in River Basins. J. Environ. Quality 38, 1924-1929.

Kronvang, B., Audet, J., Battrup-Pedersen, A., Jensen, H.S., Larsen, S.E. 2012. Phosphorus load to surface water from bank erosion in a Danish lowland river basin. J. Environ. Qual. 41, 304–313.

Levin, G., Jepsen, M.R. and Blemmer, M. 2012. Basemap. Technical Report from DCE – Danish Centre for Environment and Energy no. 11.

Morgan, R.P.C. 2005. Soil Erosion and Conservation. 3rd Ed. Blackwell Publishing, Oxford, UK. 304 p.

Møller, A.B., Beucher, A., Iversen, B.V., Greve, M.H. 2018. Predicting artificially drained areas by means of a selective model ensemble. Geoderma 320, 30-42.

Olesen, J.E., Børgesen, C.D., Jabloun, M., Wachiniew, P., Bar, D., Zurek, A., Hansen, A.L., Refsgaard, J.C., Bosshard, T. 2017. Scenario analyses of spatially differentiated N measures in catchments under future climate and land use. BONUS SOILS2SEA Deliverable 2.3. Geological Survey of Denmark and Greenland, Copenhagen, September 2017, www.SOILS2SEA.eu

Olsen, S.R., Cole, C.V., Watanabe, F.S., Dean, L.A. 1954. Estimation of available phosphorus in soils by extraction with sodium bicarbonate. Circular 939. United States Department of Agriculture, Washington DC.

Onnen, N., Heckrath, G. J., Stevens, A., Olsen, P., Greve, M. B., Kronvang, B., Van Oost, K. 2018. Distributed water erosion modelling at fine spatial resolution on a national scale in Denmark. *To be submitted* Geomorphology.

Panagos, P., Borrelli, P., Meusberger, K., Alewell, C., Lugato, E., Montanarella, L. 2015. Estimating the soil erosion cover-management factor at the European scale. Land Use Policy 48, 38-50.

Quinton, J.N., Catt, J.A., Hess, T.M. 2001. Selective removal of phosphorus from soil. Journal of Environmental Quality 30, 538-545.

Renard, K.G., Foster, G.R., Weesies, G.A., McCool, D.K. and Yoder, D.C. 1997. Predicting soil erosion by water: A guide to conversation planning with the Revised Universal Soil Loss Equation (RUSLE). United States Department of Agriculture. Agriculture Handbook Number 703.

Rosenkranz, B., Frederiksen, P., 2011. Quality assessment of the Danish Elevation Model (DK-DEM). National Survey and Cadastre—Denmark, technical report series number 12.

Rubæk, G.H., Kristensen, K., Olesen, S.E., Østergaard, H.S., Heckrath, G. 2013. Phosphorus accumulation and spatial distribution in agricultural soils in Denmark. Geoderma 209, 241-250.

Schoumans, O.F., Chardon, W.J., Bechmann, M. et al. 2014. Mitigation options to reduce phosphorus losses from the agricultural sector and improve surface water quality: A review. Science of the Total Environment 469, 1255-1266.

Van Oost, K., Govers, G., Van Muysen, W., Quine, T.A., 2000. Modeling translocation and dispersion of soil constituents by tillage on sloping land. Soil Science Society of America Journal 64, 1733-1739.

Verheijen, F.G.A., Jones, R.J.A., Rickson, R.J., Smith, C.J., 2009. Tolerable versus actual soil erosion rates in Europe. Earth-Science Reviews 94, 23-48.

The present work has been carried out within the project 'Reducing nutrient loadings from agricultural soils to the Baltic Sea via groundwater and streams (BONUS SOILS2SEA)', which has received funding from BONUS, the joint Baltic Sea research and development programme (Art 185), funded jointly by the EU and national funding agencies: Innovation Fund Denmark, The Swedish Environmental Protection Agency (Naturvådsverket), The Polish National Centre for Research and Development, The German Ministry for Education and Research (Bundesministerium für Bildung und Forschung), and The Russian Foundation for Basic Research (RFBR).